# 3D MODELING OF SPHERICAL WAVE REFLECTION ON LAYERED MEDIA WITH ROUGH INTERFACES

S. Pinson Laboratório de Vibração e Acústica, UFSC, Florianopolis, Brazil
J. Cordioli Laboratório de Vibração e Acústica, UFSC, Florianopolis, Brazil

## 1 INTRODUCTION

To perform sediment characterization by acoustics, the seafloor is generally approximated as a stack of layers with flat interfaces. In Ref. 1, the sediment sound-speed profiles have been calculated on real data using the image source method. The data used were acquired by the NURC in 2009 during the CLUTTER09 experiment. A source and a horizontal array of hydrophones were towed by an Autonomous Underwater Vehicle (AUV) 12 m above the seafloor. The source frequency band was 1600-3500 Hz. Sound-speed profiles have been calculated every 5 m over a total distance of 14 km. Results showed strong variabilities from one measurement to another. Among the possible reasons to explain those instabilities, there is a strong suspicion on the interface roughness responsibility. So to evaluate roughness influence on sound-speed profile characterization, it is necessary to model the acoustic response of a layered media with rough interfaces. Also, the model needs to be in 3D because 3D effects might play a significant role.

The literature about roughness scattering is very abundant but existing models are often statistical to assess scattering strength (or scattering cross section)[2–7]. For deterministic modeling of a spherical wave reflection on rough interfaces, existing models are generally limited to a single interface (using the Kirchhoff approximation)[8,9] or with a high computational cost (using finite-difference method)[10]. In Ref. 11 the wave propagation in range dependent media is modeled by combining the ray theory with the Kirchhoff approximation. In this communication, a similar approach is used and the three main approximations are: the tangent-plane approximation, the Born approximation (multiple reflection between interfaces are neglected) and flat-interface approximation for the transmitted waves.

The environmental configuration for the synthetic data is first described in section 2 before detailing the 3D data modeling algorithm in section 3. In section 4 the results of simulated signals are analyzed.

## 2 ENVIRONMENTAL CONFIGURATION

The numerical experiment consists in a bistatic configuration with one point source and one receiver 20 m apart and 10 m above the first interface. The source signal has a Gaussian envelope with a 1 kHz central frequency and a bandwidth of 600 Hz. Thus, the pulse duration corresponds to a 4 m length in water that provides a layer thickness resolution of about 2 m. In the time domain, the emitted pulse maximum amplitude is set to 1 at 1 m far from the source. The sampling frequency is set to 12 kHz.

The layered media is modeled by 3 layers which geoacoustic parameters are defined in table 1. In the method described next section, the model geometry is defined by the layer interfaces. Their mean planes are parallel between each other, 120 m wide and 150 m long (figure 1). The spatial sampling used to define the roughness height is set to 2.5 cm.

Interface roughnesses between the layer are generated such that the spacial power spectrum has a "Von Karman" spectrum form[12]:

$$W_2(k_x, k_y) = \frac{w_2}{(k_x^2 + k_y^2 + 1/L^2)^{\gamma_2/2}}\,, \tag{1}$$

where $k_x$ and $k_y$ are the horizontal wavenumbers, $2\pi L$ is the roughness correlation length, $\gamma_2$ the spectral exponent, and $w_2$ is the spectral strength. Values for $L$ and $\gamma_2$ are fixed respectively to 10 m and 3, and the spectral strength is set to $w_2 = 3.18 \times 10^{-4}$. With these parameters, the root mean square (rms) roughness height is $\zeta_{rms}$ =14 cm. The rms roughness height $\zeta_{rms}$ is given by:

$$\zeta_{rms}^2 = \frac{2\pi w_2}{(\gamma_2 - 2)\, L^{-(\gamma_2 - 2)}} \,. \tag{2}$$

The rms roughness height is smaller than the wavelength at the central frequency (1.5 m in water) but important enough to play a significant role on interface wave reflections.

| Layer thickness | Sound speed (m/s) | Density (kg/m$^3$) |
|---|---|---|
| Water | 1500 | 1000 |
| 3 m | 1490 | 1100 |
| 7 m | 1550 | 1300 |
| 10 m | 1600 | 1500 |
| Basement | 1700 | 1700 |

Table 1: Layered media parameters.

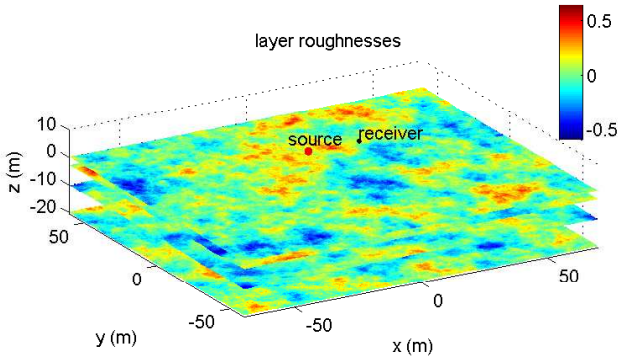


Figure 1: Example of a roughness realization for the 4 interfaces. The color scale correspond to the roughness height relative to the interface mean plane (in cm).

# 3 3D MODELING OF SPHERICAL WAVE REFLECTION ON LAYERED MEDIA WITH ROUGH INTERFACES

It is possible to show that a spherical wave reflection from a source located in $\mathbf{r}_A$ on a layered media with rough interfaces can be approximated as a sum of integrals over each interface[13]. Thus, the response at frequency $\omega$ and at the coordinate $\mathbf{r}_B$ is:

$$P(\mathbf{r}_B) = 4\pi S G_0(\mathbf{r}_B, \mathbf{r}_A) + \sum_{l=1}^{L} \mathcal{I}_{Sl}(\mathbf{r}_B) \,, \tag{3}$$

with,

$$\mathcal{I}_{Sl}(\mathbf{r}_B) \approx -4\pi S \int_{\overline{S_l}} R_{l-1l} A(\overline{\mathbf{r}_{Sl}}, \mathbf{r}_A) A(\mathbf{r}_B, \overline{\mathbf{r}_{Sl}}) \times \left( \mathrm{i}k_{l-1} \overline{\mathbf{u}^i} \cdot \mathbf{n} + \mathrm{i}k_{l-1} \overline{\mathbf{u}^r} \cdot \mathbf{n} \right) \times \exp\left\{ \mathrm{i}\omega \left( \overline{\tau^i} + \overline{\tau^r} - \frac{\zeta u_z^i + \zeta u_z^r}{c_{l-1}} \right) \right\} \frac{\mathrm{d}\overline{\mathbf{r}_{Sl}}}{n_z} , \tag{4}$$

where:

- $S$ is the source amplitude at frequency $\omega$,
- $G_0(\mathbf{r}_B, \mathbf{r}_A) = \mathrm{e}^{\mathrm{i}\omega|\mathbf{r}_B - \mathbf{r}_A|/c_0}/4\pi|\mathbf{r}_B - \mathbf{r}_A|$,
- $l$ is the layer number starting from 0 (for the water),
- $\overline{S}_l$ is the mean plane of the rough surface $S_l$,
- $\mathrm{d}\overline{\mathbf{r}_{Sl}}$ is the surface element of the mean plane $\overline{S}_l$,
- $\overline{\mathbf{r}_{Sl}}$ is a point on the mean plane $\overline{S}_l$,
- $R_{l-1l}$ is the local reflection coefficient at the interface $l$ between the layer $l-1$ and the layer $l$,
- $A(\overline{\mathbf{r}_{Sl}}, \mathbf{r}_A)$ and $A(\mathbf{r}_B, \overline{\mathbf{r}_{Sl}})$ are amplitude factors between the source $\mathbf{r}_A$ and $\overline{\mathbf{r}_{Sl}}$, and between $\mathbf{r}_{Sl}$ and the hydrophone $\mathbf{r}_B$ respectively,
- $\overline{\tau^i}$ and $\overline{\tau^r}$ are the ray travel times from $\mathbf{r}_A$ to $\overline{\mathbf{r}_{Sl}}$ and from $\overline{\mathbf{r}_{Sl}}$ to $\mathbf{r}_B$ respectively,
- $\overline{\mathbf{u}^i} = (u_x^i, u_y^i, u_z^i)$ and $\overline{\mathbf{u}^r} = (u_x^r, u_y^r, u_z^r)$ are the incidence unit vector at $\overline{\mathbf{r}_{Sl}}$ of the rays from $\mathbf{r}_A$ to $\overline{\mathbf{r}_{Sl}}$ and from $\mathbf{r}_B$ to $\overline{\mathbf{r}_{Sl}}$ respectively,
- $\mathbf{n} = (n_x, n_y, n_z)$ is the normal to the rough interface,
- $\zeta$ is the roughness height at coordinate $\overline{\mathbf{r}_{Sl}}$,
- $c_{l-1}$ is the $l-1$ layer sound speed.

Equation 4 has a convenient form for numerical evaluation. One can calculate the ray paths, geometric divergence and transmission coefficient through previous interfaces from the source and the receiver to the mean plane, and apply a correction factor in the travel times to include the roughness. All this quantities are frequency independent so that they can be calculated before the integration at a given frequency.

The amplitude factor $A(\overline{\mathbf{r}_{Sl}}, \mathbf{r}_A)$ includes the geometric divergence and the down-going transmission coefficients from the source $\mathbf{r}_A$ to $\overline{\mathbf{r}_{Sl}}$:

$$A(\overline{\mathbf{r}_{Sl}}, \mathbf{r}_A) \approx \left| \frac{c_l J(\mathbf{r}_A)}{c_0 J(\overline{\mathbf{r}_{Sl}})} \right|^{1/2} \times \prod_{p=1}^{q} T_{p-1p} , \tag{5}$$

where $T_{p-1p}$ is the transmission coefficient between layers $p-1$ and $p$, and the Jacobian of the ray is[14]:

$$J(\mathbf{r}) = \begin{vmatrix} \frac{\partial x}{\partial s} & \frac{\partial x}{\partial \theta_0} & \frac{\partial x}{\partial \psi_0} \\ \frac{\partial y}{\partial s} & \frac{\partial y}{\partial \theta_0} & \frac{\partial y}{\partial \psi_0} \\ \frac{\partial z}{\partial s} & \frac{\partial z}{\partial \theta_0} & \frac{\partial z}{\partial \psi_0} \end{vmatrix} \tag{6}$$

where $\theta_0$ is the ray incidence angle at the origin $\mathbf{r}_A$ and $\psi_0$ is its azimuth at the origin. The calculation of $A(\mathbf{r}_B, \overline{\mathbf{r}_{Sl}})$ is done in the same way with the transmission coefficient $T_{pp-1}$ between layers $p$ and $p-1$. The ray travel times are obtained by:

$$\overline{\tau} = \int \frac{1}{c(s)} \mathrm{d}s , \tag{7}$$

where $s$ is the coordinate along the ray path between $\overline{\mathbf{r}_{Sl}}$ and $\mathbf{r}_A$.

To calculate the ray paths, the method described by Langston[15] is used. It consists in the following steps:

1. send a ray parametrized by the angles $\theta_0$ and $\psi_0$ from the source or receiver location,
2. calculate its intersection coordinate on next interface,
3. calculate the transmission coefficient and the Snell's ray refraction,
4. iterate 2 and 3 to the last interface,
5. calculate reflection coefficient $R_{l-1l}$ for the ray coming from the source $\mathbf{r}_A$.

For a given ray with parameters $(\theta_0, \psi_0)$, two other rays have to be sent with parameters $(\theta_0 + \delta\theta, \psi_0)$ and $(\theta_0, \psi_0 + \delta\psi)$ in order to evaluate numerically the derivatives in the Jacobian (Equation 6). Note that, using Langston's method, interface mean planes do not have to be parallel between each other. In that case, the coordinate system in $\mathcal{I}_{Sl}$ must be rotated such that the $z$ axis is normal to the mean plane.

The plane wave reflection coefficient and the transmission coefficient are obtained by[16]:

$$\begin{aligned} R_{l-1l} &= \frac{\frac{\rho_l c_l}{|\mathbf{u}_l \cdot \mathbf{n}|} - \frac{\rho_{l-1} c_{l-1}}{|\mathbf{u}_{l-1} \cdot \mathbf{n}|}}{\frac{\rho_l c_l}{|\mathbf{u}_l \cdot \mathbf{n}|} + \frac{\rho_{l-1} c_{l-1}}{|\mathbf{u}_{l-1} \cdot \mathbf{n}_p|}} , \\ T_{p-1p} &= \frac{2\frac{\rho_p c_p}{|\mathbf{u}_p \cdot \mathbf{n}_p|}}{\frac{\rho_p c_p}{|\mathbf{u}_l \cdot \mathbf{n}_p|} + \frac{\rho_{p-1} c_{p-1}}{|\mathbf{u}_{p-1} \cdot \mathbf{n}_p|}} , \end{aligned} \tag{8}$$

where $|\mathbf{u}_{l-1} \cdot \mathbf{n}|$ and $|\mathbf{u}_l \cdot \mathbf{n}|$ are the cosines of the incidence angle before and after the interface.

At this step an issue remains to address. For a given ray parametrized by the angles $\theta_0$ and $\psi_0$, one does not master where the ray intersects the interface for which the roughness is predefined on a regular mesh. The figure 2 illustrates the issue. Lines represent many rays sent from the source or receiver to the interface, and the dots represent the regular mesh for which the roughness has been generated.

This issue is solved by noticing that quantities related to the mean plane in equation 4 vary smoothly. So one can send many rays to the mean plane and then interpolate all the ray parameters (travel time to the mean plane, incidence unit vector, transmission coefficients and geometric divergence) in equation 4 on the predefined roughness mesh. Then, $\zeta$ and $\mathbf{n}$ being known, one can apply the travel time correction $\zeta u_z / c_{l-1}$ due to the roughness and calculate the local reflection coefficient.

The figure 3 illustrates the interpolation for the ray geometric divergence from the receiver on the fourth interface of the configuration described in section 2. In this case, rays are sent to cover the predefined mean plane with a 50 cm sample length in $x$ and $y$. Ray parameters $\theta_0$ and $\psi_0$ are calculated to reach that grid as if there were no ray refraction. Of course, due to ray refraction, rays do not reach those points and leak from the grid but it is sufficient to cover the predefined roughness grid and interpolate the values (the boundary of the roughness mesh is displayed by the black rectangle in figure 3).

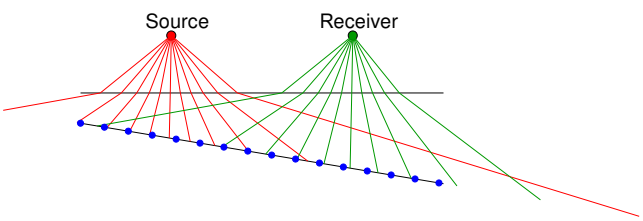


Figure 2: Rays sent from the source and the receiver to the interface. Dots represent the regular mesh for which the roughness has been generated.

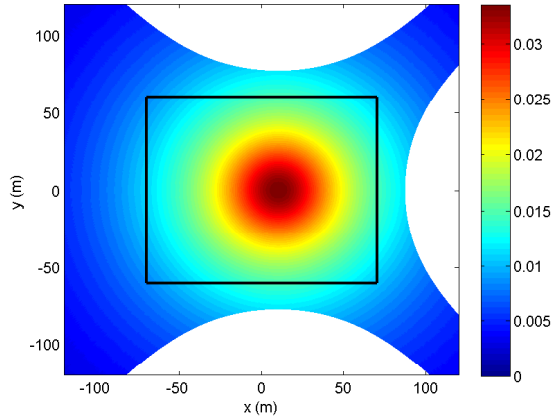


Figure 3: Geometric divergence of rays sent from the receiver to cover the fourth interface mean plane of the configuration described in section 2. Ray parameters $\theta_0$ and $\psi_0$ are calculated to reach a grid with a 50 cm sample length in $x$ and $y$ as if there were no ray refraction. Ray intersections with that plane actually do not match with that grid and leak from it because of the refraction. The black rectangle represent the boundary of the predefined roughness grid where ray parameters have to be interpolated.

# 4 RESULTS

A signal is first simulated with flat interfaces (figure 4a). One can identify the four reflections of the four interfaces and a weak backscattering after $t = 80$ ms. The backscattering comes from the diffraction at the interface boundaries. For comparison, another signal is calculated by a numerical evaluation of the Sommerfeld integral, the exact analytical solution of the reflection of a spherical wave on layered media[17]:

$$P_0^r(\mathbf{r}_B, \mathbf{r}_A, \omega) = \mathrm{i}k \int_0^{\pi/2-\mathrm{i}\infty} \mathrm{J}_0(|r_B - r_A| k \sin\theta) R(\theta, \omega) \times \mathrm{e}^{\mathrm{i}k(z_A+z_B)\cos\theta} \sin\theta \mathrm{d}\theta \,, \tag{9}$$

where $r = \sqrt{x^2 + y^2}$, $\theta$ is the angle of incidence, $k$ the wave number and $\mathrm{J}_0$ is the zeroth order Bessel function of the first kind. Because this integral is the result of plane wave decomposition, the term $R(\theta, \omega)$ is the plane wave reflection coefficient and can be computed for an arbitrary layering of fluid or elastic media[16].

Results from the two models are very similar and the comparison is done on their difference in figure 4b (the vertical scale is exaggerated by a factor of 10 compared to figure 4a). The differences between the two models are mainly explained by the presence of multiple reflections present in the simulation from the Sommerfeld integral simulation. Also it appears that interface echoes themselves (at times $t$ =19, 22, 30 and 41 ms) present some small differences. Note that multiple reflections are very weak in amplitude. Indeed, the order of magnitude of the reflection coefficients from one layer to another is $\mathcal{O}(0.1)$ so the order of magnitude of the first multiple reflection is $\mathcal{O}(10^{-3})$.

The results from simulations with rough interfaces is shown in figures 4c and 4d for two different roughness realizations. As for the flat interface case, one can identify the four interface echoes. But in these cases, echo amplitudes are affected by the roughness. The cause of these amplitude variations is probably a focusing/defocusing effect from large scale roughness oscillations. Moreover, one can see the incoherent backscattering between and after the interface echoes. This backscattering is only reliable before $t = 80$ ms because of the domain boundary diffraction.

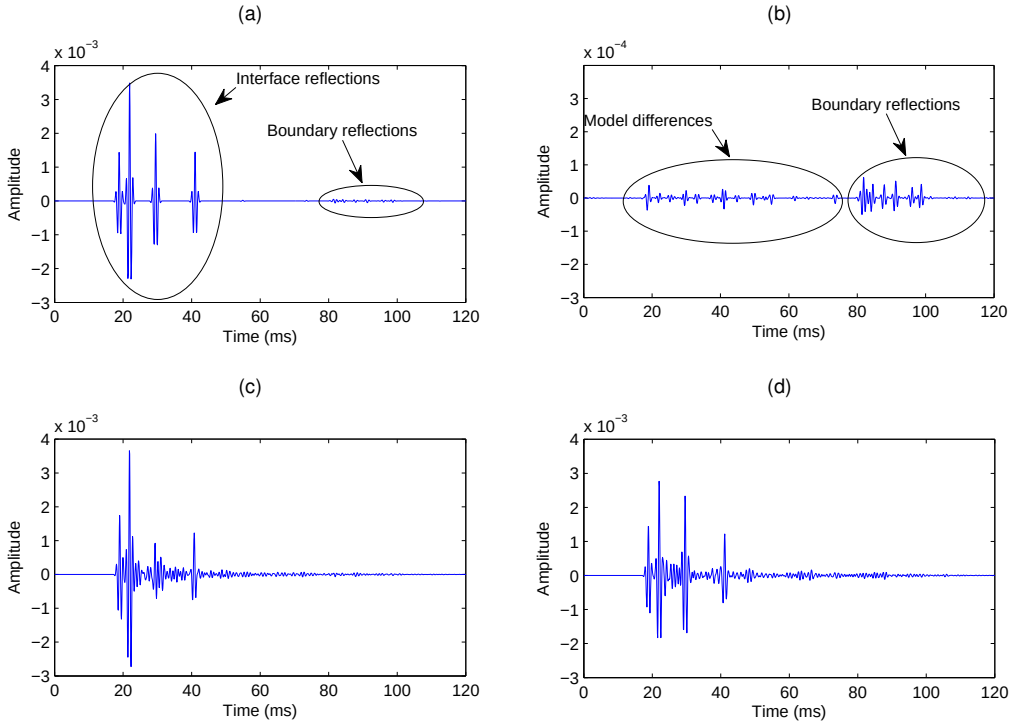


Figure 4: (a) Simulated signal with flat interfaces. (b) Difference between the simulated signal and the numerical evaluation of the Sommerfeld integral (the vertical scale is exaggerated by a factor of 10). (c) and (d) Simulated signals for two different realizations of the roughness.

# 5 CONCLUSION

A 3D model of a wave reflection on layered media with rough interfaces has been developed. The comparison with a simulation using Sommerfeld integral in the case of flat interfaces shows a good agreement. The 3D modeling neglect multiple reflections between interfaces but with low impedance contrasts, those multiples are negligible. In future works, the model will be used to study roughness influence on sound-speed profile measurement when using a source and a linear array of hydrophones.

# 6 ACKNOWLEDGMENTS

This work is supported by the CAPES (Coordenação de Aperfeiçoamento de Pessoal de Nível Superior from Brazil) through the young talent funding and partially funded by Wavetech company. The authors would like to thank Derek Olson for his help on the rough surface simulation.

# 7 REFERENCES

1. S. Pinson, L. Guillon, and C.W. Holland, 'Range dependent sediment sound speed profile measurements using the image source method', J. Acoust. Soc. Am., 134:156–165, 2013.
2. L. Guillon and X. Lurton, 'Backscattering from buried sediment layers: The equivalent input backscattering strength model', J. Acoust. Soc. Am., 109(1):122–132, 2001.
3. A.N. Ivakin, 'Models for seafloor roughness and volume scattering', In OCEANS'98 Conference Proceedings, volume 1, pages 518–521. IEEE, 1998.
4. A.N. Ivakin, 'A unified approach to volume and roughness scattering', J. Acoust Soc. Am.,

103(2):827–837, 1998.

5. D.R. Jackson, R.I. Odom, M.L. Boyd, and A.N. Ivakin, 'A geoacoustic bottom interaction model (GABIM)', IEEE Journal of Oceanic Engineering, 35(3):603–617, 2010.
6. J.Y. Liu, P.C. Hsueh, and C.F. Huang, 'Coherent reflection of acoustic plane wave from a rough seabed, with a random sediment layer overlying an elastic basement', Oceanic Engineering, IEEE Journal of, 27(4):853–861, Oct 2002.
7. C. Wu and X. Zhang, 'Second-order perturbative solutions for 3-d electromagnetic radiation and propagation in a layered structure with multilayer rough interfaces', IEEE Journal of Selected Topics in Applied Earth Observations and Remote Sensing, 8(1):180–194, Jan 2015.
8. E. Pouliquen, A.P. Lyons, and N.G. Pace, 'Penetration of acoustic waves into rippled sandy seafloors', J. Acoust. Soc. Am., 108(5):2071–2081, 2000.
9. E. Pouliquen, A.P. Lyons, and N.G. Pace, 'The helmholtz–kirchhoff approach to modeling penetration of acoustic waves into rough seabeds', J. Acoust. Soc. Am., 104(3):1762–1762, 1998.
10. W. Makinde, N. Favretto-Cristini, and E. De Bazelaire, 'Numerical modelling of interface scattering of seismic wavefield from a random rough interface in an acoustic medium: comparison between 2d and 3D cases', Geophysical prospecting, 53(3):373–397, 2005.
11. V. Cerveny, Seismic Ray Theory, pp 417–449 Cambridge University Press, 2001.
12. D. Jackson and M.D. Richardson, High-frequency seafloor acoustics, pp 475–479 Springer, New York, 2007.
13. S. Pinson and J. Cordioli, 'Spherical wave reflection on layered media with rough interfaces. I. 3D modeling'. J. Acoust. Soc. Am., Submitted.
14. F.B. Jensen, W.A. Kupperman, M.B. Porter, and H. Shmidt, Computational ocean acoustics, pp 156–168 American Institute of Physics, New York, 1994.
15. C.A. Langston, 'The effect of planar dipping structure on source and receiver responses for constant ray parameter', Bulletin of the Seismological Society of America, 67(4):1029–1050, 1977.
16. L. Brekhovskikh and Y. Lysanov, Fundamentals of Ocean Acoustics, pp 61–79, Springer-Verlag, Berlin, 1991.
17. L. Brekhovskikh and O. Godin. Acoustics of layered media. II : point sources and bounded beams, pp 1–15. Springer-Verlag, Berlin, 1999.